Sampled-Data PID Control and Anti-aliasing Filters*

Marian J. Blachuta and Rafal T. Grygiel
Department of Automatic Control, Silesian University of Technology
Poland

1. Introduction

Consider a typical configuration of the sampled-data control system. It consists of the plant to be controlled, a sampler, a discrete-time controller and a zero-order hold. Disturbance can be seen as an integral part of the plant so that the plant is characterized by the control path responsible for control signal influence on the output and the disturbance. The system output is usually sensed by sensors whose output signal can be corrupted by noise. Sometimes analog filters are put between the analog sensor output signal and sampler. In the control literature

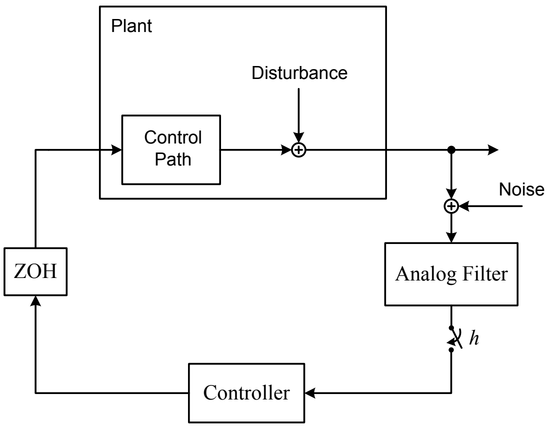

Fig. 1. General control system diagram

(Åström and Wittenmark, 1997; Feuer and Goodwin, 1996) strong belief is expressed, that filters are necessary prior to sampling to guarantee correct digital signal processing and control. This belief is usually supported by heuristic speculations based on Shannon-Kotelnikov Reconstruction Theorem, e.g. (Jerri, 1977), which states that in order to reconstruct the signal $s(t)$ from its samples $s(ih)$, $-\infty < i < \infty$, the sampling frequency should be at least twice the highest frequency component in the signal. Since the spectra of physical signals often stretch on infinite frequency range, this gives rise to the idea of so called anti-aliasing filters that cut off the portion of frequency spectrum lying outside the region determined by that theorem.

*This work has been granted by the Polish Ministry of Science and Higher Education from funds for years 2008-2011

It should, however, be stressed that no proofs are available concerning the necessity of anti-aliasing filters in sampled-data systems, and no statements can be found with regard to the consequences of the lack of such filters.
Anti-aliasing filters usually take the form of Butterworth filters whose cutoff frequency equals to the so called Nyquist frequency $\omega_N = \pi/h$, which is depending solely on sampling period h. As an alternative, so called integrating or averaging samplers are considered (Blachuta & Grygiel, 2008a;b; Feuer and Goodwin, 1996; Goodwin et al., 2001; Steinway and Melsa, 1971; Shats and Shaked, 1989).
In (Blachuta & Grygiel, 2008a;b) we studied the impact of antialiasing filters for pure signal processing, while in (Blachuta & Grygiel, 2009b) the context of discrete-time LQG control was discussed. The statement was made, that there is no reason for using them in the noiseless case, and practically they find no use in the case of noisy measurements. The best results in the latter case are obtained when the continuous-time output is passed through a continuous-time Kalman filter, which depends rather on disturbance and noise characteristics than the sampling period, before being sampled. Similar results were observed in PID control systems (Blachuta & Grygiel, 2009a;b;c)and (Blachuta & Grygiel, 2010)
In this chapter we summarize these results and compare them with LQG minimum-variance benchmark control using simple, but representative examples.

2. Analog part of the system

2.1 Plant, disturbance and noise model

The model of system displayed in Fig. 1 is presented in Fig. 2, where $K_c(s)$ is the transfer function of control path of the plant, while $K_d(s)$ and $K_n(s)$ represent filters forming stochastic disturbance and noise, respectively. $K_f(s)$ stands for a continuous-time filter.

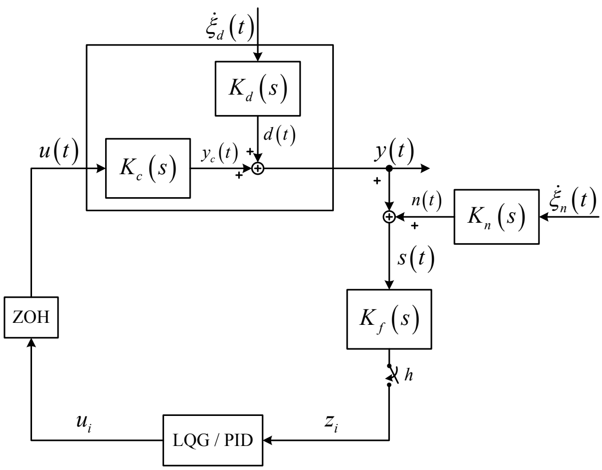

Fig. 2. Control system

The entire continuous-time system can be modeled in state-space as follows:

$$\dot{\boldsymbol{x}}(t) = \boldsymbol{A}\boldsymbol{x}(t) + \boldsymbol{b}u(t) + \boldsymbol{C}\dot{\boldsymbol{\xi}}(t), \tag{1}$$

$$y(t) = \boldsymbol{d}_y'\boldsymbol{x}(t), \tag{2}$$

$$s(t) = \boldsymbol{d}_s'\boldsymbol{x}(t), \tag{3}$$

$$z(t) = \boldsymbol{d}'\boldsymbol{x}(t), \tag{4}$$

where:

$$\boldsymbol{A} = \begin{bmatrix} \boldsymbol{A}_c & \boldsymbol{0} & \boldsymbol{0} & \boldsymbol{0} \\ \boldsymbol{0} & \boldsymbol{A}_d & \boldsymbol{0} & \boldsymbol{0} \\ \boldsymbol{0} & \boldsymbol{0} & \boldsymbol{A}_n & \boldsymbol{0} \\ \boldsymbol{b}_f\boldsymbol{d}_c' & \boldsymbol{b}_f\boldsymbol{d}_d' & \boldsymbol{b}_f\boldsymbol{d}_n' & \boldsymbol{A}_f \end{bmatrix}, \quad \boldsymbol{C} = \begin{bmatrix} \boldsymbol{0} & \boldsymbol{0} \\ \boldsymbol{c}_d & \boldsymbol{0} \\ \boldsymbol{0} & \boldsymbol{c}_n \\ \boldsymbol{0} & \boldsymbol{0} \end{bmatrix},$$

$$\boldsymbol{b} = \begin{bmatrix} \boldsymbol{b}_c \\ \boldsymbol{0} \\ \boldsymbol{0} \\ \boldsymbol{0} \end{bmatrix}, \boldsymbol{d}_y = \begin{bmatrix} \boldsymbol{d}_c \\ \boldsymbol{d}_d \\ \boldsymbol{0} \\ \boldsymbol{0} \end{bmatrix}, \boldsymbol{d}_s = \begin{bmatrix} \boldsymbol{d}_c \\ \boldsymbol{d}_d \\ \boldsymbol{d}_n \\ \boldsymbol{0} \end{bmatrix}, \boldsymbol{d} = \begin{bmatrix} \boldsymbol{0} \\ \boldsymbol{0} \\ \boldsymbol{0} \\ \boldsymbol{d}_f \end{bmatrix},$$

$$\boldsymbol{x}(t) = \begin{bmatrix} \dot{\boldsymbol{x}}_c(t) \\ \dot{\boldsymbol{x}}_d(t) \\ \dot{\boldsymbol{x}}_n(t) \\ \dot{\boldsymbol{x}}_f(t) \end{bmatrix}, \quad \dot{\boldsymbol{\xi}}(t) = \begin{bmatrix} \dot{\xi}_d(t) \\ \dot{\xi}_n(t) \end{bmatrix}.$$

Processes $\dot{\xi}_d(t)$ and $\dot{\xi}_n(t)$ are independent continuous-time white noises with zero means and covariance functions defined as unit Dirac pulse functions, i.e.:

$$\mathrm{E}\left[\dot{\xi}_d(t)\right] = 0, \qquad \mathrm{E}\left[\dot{\xi}_d(t)\dot{\xi}_d(\tau)\right] = \delta(t-\tau); \tag{5}$$

$$\mathrm{E}\left[\dot{\xi}_n(t)\right] = 0, \qquad \mathrm{E}\left[\dot{\xi}_n(t)\dot{\xi}_n(\tau)\right] = \delta(t-\tau). \tag{6}$$

2.2 Analog Filters

In the paper two types of filters are considered: Butterworth filter as the anti-aliasing filter, as well as a continuous-time Kalman filter as a filter based on signals spectra.

2.2.1 Butterworth Filter

Transfer function of the Butterworth filter has the form:

$$K_f(s) = \frac{1}{B_n\left(\frac{s}{\omega_o}\right)}, \tag{7}$$

where $B_n(*)$ is the n^{th}-degree Butterworth's polynomial and ω_o is called the cutoff frequency. In this paper ω_o will be assumed as Nyquist frequency $\omega_o = \omega_N = \frac{\pi}{h}$. The first Butterworth's polynomials are definded as follows:

$$B_1(x) = x + 1; \quad B_2(x) = x^2 + \sqrt{2} \cdot x + 1. \tag{8}$$

2.2.2 Kalman Filter

Kalman filter is the one that provides the best noise filtering under assumptions of our model. Since the noise added to the measured output is not white, the classical Kalman filter for a system consisting of disturbance and noise becomes singular. One way to overcome the problem is to replace the continuous-time filter with a discrete-time one working at a high enough sampling frequency $1/h_f$. The output of such filter could be re-sampled at lower frequency if necessary.

Very often the power spectrum $S_n(\omega)$ of noise $n(t)$, defined by transfer function $K_n(s)$, is much wider than that of the signal of interest $y(t)$. In such case it can be modeled as white noise $n(t)$

$$\mathrm{E}\left[n(t)\right] = 0, \qquad \mathrm{E}\left[n(t)n(\tau)\right] = \eta^2\delta(t-\tau); \tag{9}$$

with constant spectral density η^2 independent of frequency ω. The model of disturbances is then simplified to

$$\dot{\boldsymbol{x}}_d(t) = \boldsymbol{A}_d\boldsymbol{x}_d(t) + \boldsymbol{c}_{\boldsymbol{d}}\dot{\xi}_d(t), \tag{10}$$

$$y_{dn}(t) = \boldsymbol{d}_d'\boldsymbol{x}_d(t) + \eta\dot{\xi}_n(t), \tag{11}$$

with

$$\eta = |K_n(0)| = |\boldsymbol{d}_n'\boldsymbol{A}_n^{-1}\boldsymbol{c}_n| \tag{12}$$

The continuous-time Kalman filter is then defined by:

$$\dot{\boldsymbol{x}}_f(t) = \boldsymbol{A}_d\boldsymbol{x}_f(t) + \boldsymbol{k}_c^f\left[y_{dn}(t) - \boldsymbol{d}_d'\boldsymbol{x}_f(t)\right] \tag{13}$$

where:

$$\boldsymbol{k}_c^f = \frac{\boldsymbol{P}\boldsymbol{d}_d}{\eta^2}; \quad \boldsymbol{A}_d\boldsymbol{P} + \boldsymbol{P}\boldsymbol{A}_d' - \frac{\boldsymbol{P}\boldsymbol{d}_d\boldsymbol{d}_d'\boldsymbol{P}}{\eta^2} + \boldsymbol{c}_d\boldsymbol{c}_d' = 0. \tag{14}$$

We use this filter in the system to pass the signal $y_2(t)$ through it, i.e. we substitute $y_{dn}(t) = y_2(t)$ and receive $z(t) = \boldsymbol{d}_d'\boldsymbol{x}_f(t)$

Since only a rough characterization of noise is required and filter equations are of lower order equal to the order of disturbance model, analog filtering is greatly simplified.

3. Control algorithms

The aim of the control system is to keep the output of the system close to the reference value $y^r(t) = 0$, i.e. to make the error $e(t) = y^r(t) - y(t)$ small. Since standard deviation is a good measure of the expected magnitude, the quality of the control systems will be assessed based on standard deviation of output and control signals. To this end, appropriate variations should be calculated.

3.1 PID controller

Discrete-time PID controller defined by transfer function:

$$K_{reg}(\mathrm{z}) = \frac{U(\mathrm{z})}{E(\mathrm{z})} = k_P\left(1 + \frac{h}{T_I}\frac{\mathrm{z}}{\mathrm{z}-1} + \frac{T_D}{h}\frac{\mathrm{z}-1}{\mathrm{z}}\right) \tag{15}$$

can be presented in the state-space form, assuming $e_i = -z_i$, as follows:

$$\boldsymbol{x}_{i+1}^r = \boldsymbol{F}_r\boldsymbol{x}_i^r - \boldsymbol{g}_r z_i, \tag{16}$$

$$u_i = \boldsymbol{d}_r'\boldsymbol{x}_i^r - e_r z_i, \tag{17}$$

P	$k_P = \frac{T}{k \cdot L}$	–	–
PI	$k_P = 0.9\frac{T}{k \cdot L}$	$T_I = 3.33 \cdot L$	–
PID	$k_P = 1.2\frac{T}{k \cdot L}$	$T_I = 2 \cdot L$	$T_D = 0.5 \cdot L$

Table 1. QDR PID controller settings

where:

$$\boldsymbol{F}_r = \begin{bmatrix} 1 & 0 \\ 0 & 0 \end{bmatrix}, \qquad \boldsymbol{g}_r = \begin{bmatrix} 1 \\ 1 \end{bmatrix}, \qquad \boldsymbol{d}_r = \begin{bmatrix} k_P \frac{h}{T_I} \\ -k_P \frac{T_D}{h} \end{bmatrix}, \qquad e_r = k_p \left[1 + \frac{h}{T_I} + \frac{T_D}{h} \right] \tag{18}$$

3.1.1 QDR controller settings

There are several methods to find continuous-time PID controller settings. Perhaps the simplest one is the so called QDR (Quarter Decay Ratio) method, which is based on lag-delay approximation of the plant. We adapt this method to sampled-data controller using a continuous-time approximation of the discrete-time system consisting of ZOH, plant, filter and sampler. Moreover, a lag-delay approximation $G_{OL}(s)$ of the control path including respective filter, $K_{OL}(s) = K_c(s)K^f(s)$, is used.

$$G_{OL}(s) = \frac{k}{Ts+1}\mathrm{e}^{-s\tau}. \tag{19}$$

The parameters of $G_{OL}(s)$ can be determined by several methods based on the step response of $K_{OL}(s)$. One of them, called "two points method", relies on two time instants, t_1 and t_2, at which the step response reaches the values 63.2% and 28.3% of the steady state, respectively. We then have:

$$T = 1.5\,(t_1 - t_2)\,, \qquad \tau = t_1 - T. \tag{20}$$

Then the QDR settings (Goodwin et al., 2001) are taken from Table 1 where L accounts for ZOH and sampler as follows:

$$L = \tau + \frac{h}{2}, \tag{21}$$

which corresponds to the $h/2$ delay approximation of ZOH.

3.1.2 Optimal PID controller

QDR controller settings do not depend on disturbance and noise characteristics. Therefore optimal controllers settings $\hat{\boldsymbol{p}} = \begin{bmatrix} \hat{k}_P & \hat{T}_I^j & \hat{T}_D^j \end{bmatrix}'$ will be chosen as the ones minimizing the output variance of the controlled system:

$$\hat{\boldsymbol{p}} = \arg\min_{\boldsymbol{p}} \operatorname{var}\{y_i\} \tag{22}$$

where the variance $\operatorname{var}\{y_i\}$ is determined by the formuale in (24) - (28) that take disturbance and noise characteristics into account. Denoting $\hat{\boldsymbol{p}}^j = \begin{bmatrix} \hat{k}_P^j & \hat{T}_I^j & \hat{T}_D^j \end{bmatrix}'$ at j-th stage of the minimization procedure, the computation stops when:

$$\|\hat{\boldsymbol{p}}^j - \hat{\boldsymbol{p}}^{j-1}\| < \varepsilon \text{ where } \varepsilon = 0.01 \tag{23}$$

In the above, Powell method of extremum seeking, amended with a procedure determining the range of stable values of parameters at each direction, can be used. The parameters resulting from QDR tuning can then be chosen as an initial guess.

3.1.3 PID Control System Assessment

The output and control variances are as follows:

$$\sigma_y^2 = \text{var}\{y_i\} = \boldsymbol{d}_y' \boldsymbol{V}^p \boldsymbol{d}_y, \tag{24}$$

$$\sigma_u^2 = \text{var}\{u_i\} = \boldsymbol{d}_r' \boldsymbol{V}^r \boldsymbol{d}_r + e_r \boldsymbol{d}' \boldsymbol{V}^p \boldsymbol{d} e_r - \boldsymbol{d}_r' \boldsymbol{V}^{rp} \boldsymbol{d} e_r - e_r \boldsymbol{d}' \boldsymbol{V}^{pr} \boldsymbol{d}_r, \tag{25}$$

where the covariance matrix $\boldsymbol{V}$

$$\boldsymbol{V} = \text{E}\left\{ \begin{bmatrix} \boldsymbol{x}_i \\ \boldsymbol{x}_i^r \end{bmatrix} \begin{bmatrix} \boldsymbol{x}_i' & \boldsymbol{x}_i^{r\prime} \end{bmatrix} \right\} = \begin{bmatrix} \boldsymbol{V}_i^p & \boldsymbol{V}_i^{pr} \\ \boldsymbol{V}_i^{rp} & \boldsymbol{V}_i^r \end{bmatrix} \tag{26}$$

is a solution of

$$\boldsymbol{V} = \boldsymbol{\Phi} \boldsymbol{V} \boldsymbol{\Phi}' + \boldsymbol{\Lambda} \boldsymbol{W} \boldsymbol{\Lambda}' \tag{27}$$

with

$$\boldsymbol{\Phi} = \begin{bmatrix} (\boldsymbol{F} - \boldsymbol{g} e_r \boldsymbol{d}') & \boldsymbol{g} \boldsymbol{d}_r' \\ -\boldsymbol{g}_r \boldsymbol{d}' & \boldsymbol{F}_r \end{bmatrix}, \quad \boldsymbol{\Lambda} = \begin{bmatrix} \boldsymbol{I} \\ 0 \end{bmatrix} \tag{28}$$

3.2 MV LQG control law

The best control accuracy is achieved when using the optimal Minimum-Variance sampled-data LQG controller which will be used as a benchmark to assess PID control quality.

3.2.1 Controller

LQG control problem with a continuous performance index J is formulated, where

$$J = \lim_{N \to \infty} \text{E} \frac{1}{Nh} \int_0^{Nh} \{y^2(t) + \lambda u^2(t)\} dt. \tag{29}$$

Setting $\lambda = 0$ defines a MV sampled-data LQG problem. Since noise influences only state estimate $\hat{\boldsymbol{x}}_{i|i}$ and not the control law, being itself a linear function of $\hat{\boldsymbol{x}}_{i|i}$ the above sampled data control problem can be reformulated as follows.
The problem defined by modulation equation

$$u(t) = u_i, \text{ for } t \in (ih, ih + h], \ i = 0, 1, \ldots, \tag{30}$$

state equation

$$\dot{\boldsymbol{x}}_p(t) = \boldsymbol{A}_p \boldsymbol{x}_p(t) + \boldsymbol{b}_p u(t) + \boldsymbol{c}_p \dot{\xi}(t), \tag{31}$$

$$y(t) = \boldsymbol{d}_p' \boldsymbol{x}_p(t), \tag{32}$$

where:

$$\boldsymbol{A}_p = \begin{bmatrix} \boldsymbol{A}_c & \boldsymbol{0} \\ \boldsymbol{0} & \boldsymbol{A}_d \end{bmatrix}, \quad \boldsymbol{b}_p = \begin{bmatrix} \boldsymbol{b}_c \\ \boldsymbol{0} \end{bmatrix}, \quad \boldsymbol{c}_p = \begin{bmatrix} \boldsymbol{0} \\ \boldsymbol{c}_d \end{bmatrix},$$

$$\boldsymbol{d}_p = \begin{bmatrix} \boldsymbol{d}_c \\ \boldsymbol{d}_d \end{bmatrix}, \quad \boldsymbol{x}_p(t) = \begin{bmatrix} \boldsymbol{x}_c(t) \\ \boldsymbol{x}_d(t) \end{bmatrix}, \quad \dot{\xi}(t) = \dot{\xi}_d(t),$$

and feedback signal z_i, is equivalent with the following discrete-time problem

$$\boldsymbol{x}_{i+1}^p = \boldsymbol{F}_p \boldsymbol{x}_i^p + \boldsymbol{g}_p u_i + \boldsymbol{w}_i^p, \quad (33)$$

$$z_i = \boldsymbol{d}_p' \boldsymbol{x}_i^p, \quad (34)$$

$$J = \lim_{N\to\infty} \mathrm{E}\, \frac{1}{N} \sum_{i=0}^{N-1} \{ \boldsymbol{x}_i^{p\prime} \boldsymbol{Q}_1 \boldsymbol{x}_i^p + 2\boldsymbol{x}_i^{p\prime} \boldsymbol{q}_{12} u_i + q_2 u_i^2 + q_w \}, \quad (35)$$

where

$$\boldsymbol{Q}_1 = \frac{1}{h} \int_0^h \boldsymbol{F}_p'(\tau) \boldsymbol{M} \boldsymbol{F}_p(\tau) d\tau, \qquad \boldsymbol{M} = \boldsymbol{d}_p \boldsymbol{d}_p',$$

$$\boldsymbol{q}_{12} = \frac{1}{h} \int_0^h \boldsymbol{F}_p'(\tau) \boldsymbol{M} \boldsymbol{g}_p(\tau) d\tau,$$

$$q_2 = \frac{1}{h} \int_0^h \boldsymbol{g}_p'(\tau) \boldsymbol{M} \boldsymbol{g}_p(\tau) d\tau + \lambda,$$

$$q_w = \boldsymbol{d}_p' \left\{ \int_0^h \int_0^\tau \boldsymbol{F}_p(\tau - s) \boldsymbol{c}_p \boldsymbol{c}_p' \boldsymbol{F}_p'(\tau - s) ds d\tau \right\} \boldsymbol{d}_p,$$

$$\boldsymbol{F}_p(\tau) = e^{\boldsymbol{A}_p \tau}, \qquad \boldsymbol{F}_p = \boldsymbol{F}_p(h), \quad (36)$$

$$\boldsymbol{g}_p(\tau) = \int_0^\tau e^{\boldsymbol{A}_p \nu} \boldsymbol{b}_p d\nu, \qquad \boldsymbol{g}_p = \boldsymbol{g}_p(h) \quad (37)$$

and $\boldsymbol{w}_i^p$ is a zero mean vector Gaussian noise with $\mathrm{E}\{\boldsymbol{w}_i^p \boldsymbol{w}_i^{p\prime}\} = \boldsymbol{W}_p$, and

$$\boldsymbol{W}_p = \int_0^h \mathrm{e}^{\boldsymbol{A}_p s} \boldsymbol{c}_p \boldsymbol{c}_p' \mathrm{e}^{\boldsymbol{A}_p' s} ds. \quad (38)$$

Vectors $\boldsymbol{x}_0^p$ and $\boldsymbol{w}_i^p$ are independent for all $i \geq 0$. The optimal control law minimizing the performance index (35) for the discrete stochastic system (33)-(34) is a linear function

$$u_i = -\boldsymbol{k}_x' \hat{\boldsymbol{x}}_{i|i}^p, \quad (39)$$

where $\hat{\boldsymbol{x}}_{i|i}^p$ denotes the Kalman filter estimate of $\boldsymbol{x}_i^p$ based on available information up to and including i from (47)-(48).The feedback gain $\boldsymbol{k}_x$,

$$\boldsymbol{k}_x' = \frac{\boldsymbol{q}_{12} + \boldsymbol{F}_p' \boldsymbol{K} \boldsymbol{g}_p}{q_2 + \boldsymbol{g}_p' \boldsymbol{K} \boldsymbol{g}_p} \quad (40)$$

depends on the positive definite solution $\boldsymbol{K}$ of the following algebraic Riccati equation:

$$\boldsymbol{K} = \boldsymbol{Q}_1 + \boldsymbol{F}_p' \boldsymbol{K} \boldsymbol{F}_p - \frac{(\boldsymbol{q}_{12} + \boldsymbol{F}_p' \boldsymbol{K} \boldsymbol{g}_p)(\boldsymbol{q}_{12} + \boldsymbol{F}_p' \boldsymbol{K} \boldsymbol{g}_p)'}{q_2 + \boldsymbol{g}_p' \boldsymbol{K} \boldsymbol{g}_p}.$$

3.2.2 Discrete-time Kalman filter

Simple instantaneous sampling with sampling period h consists in taking the values of the sampled signal at discrete time instants $t_i = ih, i = 0, 1, \ldots$. Available measurements z_i are expressed as

$$z_i = y_2(t_i). \tag{41}$$

The problem defined by measurement equation $z_i = z(ih)$ and state equation (1) is equivalent to the following discrete-time system:

$$\boldsymbol{x}_{i+1} = \boldsymbol{F}\boldsymbol{x}_i + \boldsymbol{g}u_i + \boldsymbol{w}_i, \tag{42}$$

$$z_i = \boldsymbol{d}'\boldsymbol{x}_i, \tag{43}$$

where:

$$\boldsymbol{F}(\tau) = e^{\boldsymbol{A}\tau}, \qquad \boldsymbol{F} = \boldsymbol{F}(h), \tag{44}$$

$$\boldsymbol{g}(\tau) = \int_0^{\tau} e^{\boldsymbol{A}\nu}\boldsymbol{b}d\nu, \qquad \boldsymbol{g} = \boldsymbol{g}(h) \tag{45}$$

and $\boldsymbol{w}_i$ is a zero mean vector Gaussian noise with $\mathrm{E}\left\{\boldsymbol{w}_i\boldsymbol{w}_i'\right\} = \boldsymbol{W}$, and

$$\boldsymbol{W} = \int_0^{h} \mathrm{e}^{\boldsymbol{A}s}\boldsymbol{C}\boldsymbol{C}'\mathrm{e}^{\boldsymbol{A}'s}ds. \tag{46}$$

Vectors $\boldsymbol{x}_0$ and $\boldsymbol{w}_i$ are independent for all $i \geq 0$.
The limiting Kalman filter, (Anderson & Moore, 1979), that provides $(\hat{\boldsymbol{x}}_{i|i} = \mathrm{E}\left[\boldsymbol{x}_i|\vec{\boldsymbol{z}}_i\right])$ for the discrete-time system in (42)-(43) as $i \to \infty$ has the form:

$$\hat{\boldsymbol{x}}_{i+1|i+1} = \hat{\boldsymbol{x}}_{i+1|i} + \boldsymbol{k}^f(z_{i+1} - \boldsymbol{d}'\hat{\boldsymbol{x}}_{i+1|i}), \tag{47}$$

$$\hat{\boldsymbol{x}}_{i+1|i} = \boldsymbol{F}\hat{\boldsymbol{x}}_{i|i} + \boldsymbol{g}u_i, \qquad \boldsymbol{x}_{0|-1} = 0, \tag{48}$$

where

$$\boldsymbol{k}^f = \frac{\boldsymbol{\Sigma}\boldsymbol{d}}{\boldsymbol{d}'\boldsymbol{\Sigma}\boldsymbol{d}'}, \quad \boldsymbol{\Sigma} = \boldsymbol{W} + \boldsymbol{F}\left(\boldsymbol{\Sigma} - \frac{\boldsymbol{\Sigma}\boldsymbol{d}\boldsymbol{d}'\boldsymbol{\Sigma}'}{\boldsymbol{d}'\boldsymbol{\Sigma}\boldsymbol{d}}\right)\boldsymbol{F}'. \tag{49}$$

3.2.3 MV LQG Control System Assessment

Output and control variances for systems with continuous-time filters can be expressed by following formulae:

$$\sigma_y^2 = \mathrm{var}\left\{y_i\right\} = \boldsymbol{d}_0'\boldsymbol{V}^o\boldsymbol{d}_0, \tag{50}$$

$$\sigma_u^2 = \mathrm{var}\left\{u_i\right\} = \boldsymbol{k}_x'\boldsymbol{V}^f\boldsymbol{k}_x, \tag{51}$$

where $\boldsymbol{V}^o$, $\boldsymbol{V}^f$, end $\boldsymbol{V}^{fo}$ are submatrices of matrix $\boldsymbol{V}$

$$\boldsymbol{V} = \mathrm{E}\left\{\begin{bmatrix}\boldsymbol{x}_i \\ \hat{\boldsymbol{x}}_{i|i}\end{bmatrix}\begin{bmatrix}\boldsymbol{x}_i' & \hat{\boldsymbol{x}}_{i|i}'\end{bmatrix}\right\} = \begin{bmatrix}\boldsymbol{V}^o & \boldsymbol{V}^{of} \\ \boldsymbol{V}^{fo} & \boldsymbol{V}^f\end{bmatrix} \tag{52}$$

which is a solution of the following matrix Lyapunov equation:

$$\boldsymbol{V} = \boldsymbol{\Phi}\boldsymbol{V}\boldsymbol{\Phi}' + \boldsymbol{\Omega}\boldsymbol{W}\boldsymbol{\Omega}', \tag{53}$$

with:

$$\boldsymbol{\Lambda} = (\boldsymbol{I} - \boldsymbol{k}^f \boldsymbol{d}')(\boldsymbol{F} + \boldsymbol{g}\boldsymbol{k}_x'), \qquad \boldsymbol{\Psi} = (\boldsymbol{\Lambda} + \boldsymbol{k}^f \boldsymbol{d}' \boldsymbol{g} \boldsymbol{k}_x'),$$

$$\boldsymbol{\Phi} = \begin{bmatrix} \boldsymbol{F} & \boldsymbol{g}\boldsymbol{k}_x' \\ \boldsymbol{k}^f \boldsymbol{d}' \boldsymbol{F} & \boldsymbol{\Psi} \end{bmatrix}, \qquad \boldsymbol{\Omega} = \begin{bmatrix} \boldsymbol{I} \\ \boldsymbol{k}^f \boldsymbol{d}' \end{bmatrix}.$$

4. Examples

We will study the properties of control systems for a plant having control path

$$K_c(s) = \frac{1}{(1+0.5s)^2}, \tag{54}$$

with disturbance modeled by:

$$K_d(s) = \frac{k_d}{(1+T_d s)^2}, \tag{55}$$

with $T_d = 2$ and k_d chosen such, that $\operatorname{var} d(t) = 1$. For the noise model in Fig.2 we use three different transfer functions

$$K_n^1(s) = \frac{k_n^1}{T_n^2 s^2 + 2\zeta_n T_n s + 1}, T_n = 0.05, \zeta_n = 1 \tag{56}$$

$$K_n^2(s) = \frac{k_n^2}{T_n^2 s^2 + 2\zeta_n T_n s + 1}, T_n = 0.05, \zeta_n = 0.05 \tag{57}$$

$$K_n^3(s) = k_n^3 \cdot (K_n^1(s) + K_n^2(s)) \tag{58}$$

with $k_n^i, i = 1,2,3$ chosen such that $\operatorname{var} n(t) = \sigma_n^2$. The model in eq. (56) produces a wide-band noise, the one in eq. (57) a narrow band, while the model in eq. (58) a mixed character one. Spectral density characteristics of $K_n(s)$ and $K_d(s))$ are presented in Fig. 3.

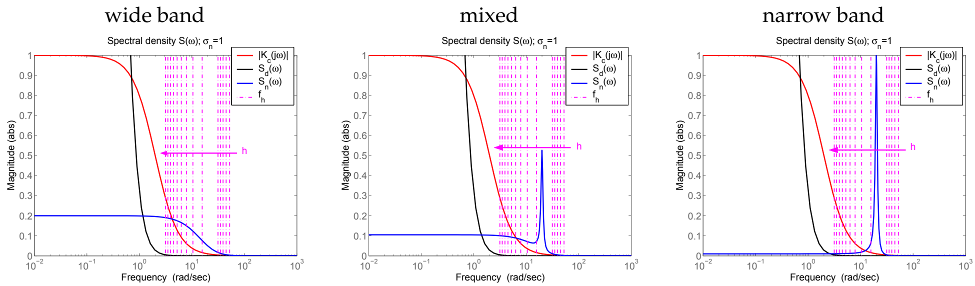

Fig. 3. Spectral density for std $\{n(t)\} = 1.0$

4.1 Open-loop results

The effect of Butterworth filter compared with continuous-time Kalman filter in the pure signal processing context is presented in Fig. 4a - b for a wide-band noise. In Fig. 4a it is clearly seen, that for small level of noise the only result is that filtration error increases with increasing sampling period h. This is due to the signal deformation caused by filtering. At high noise levels there are two effects: decreasing influence of noise with increasing sampling period accompanied by increasing deformation of the useful signal. This situation becomes greatly improved when Butterworth filter is followed by a discrete-time Kalman filter of (47)-(48), see Fig. 4b. In this figure we have $\text{std}\,(\Delta d^*) = \lim_{i\to\infty} \text{std}\,\{\Delta d^*(i)\}$, where $\Delta d^*(i)$ is the difference between actual value d_i and a sample s_i, and $\text{std}\,(\Delta s) = \lim_{i\to\infty} \text{std}\,\{\Delta s(i)\}$, where $\Delta d(i) = d_i - \hat{d}_{i|i}$ is the difference between d_i and its estimate $\hat{d}_{i|i}$ produced by the discrete-time Kalman filter These phenomena will play important role in the control context in closed loop.

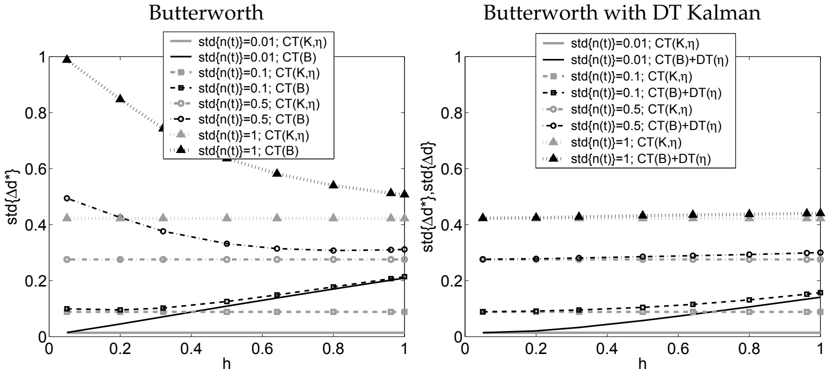

Fig. 4. Wide-band noise filtering results: CT Butterworth filter and CT Butterworth with DT Kalman compared with CT Kalman filter

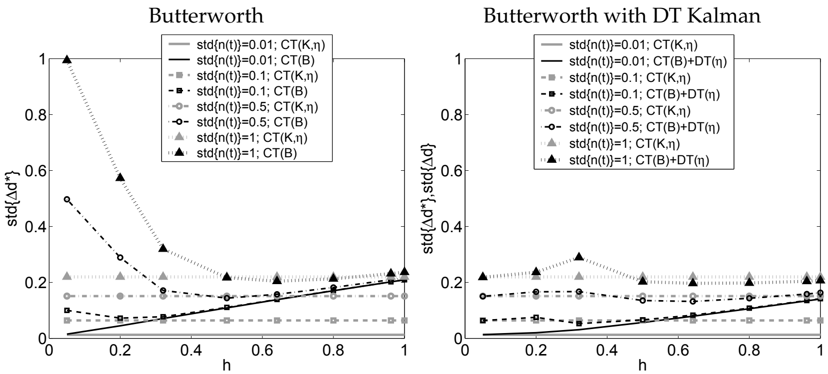

Fig. 5. Narrow-band noise filtering results: CT Butterworth filter and CT Butterworth with DT Kalman compared with CT Kalman filter

4.2 Closed-loop results

The results for PID QDR, optimal PID and LQG controlled systems are presented in figure Fig. 6 as functions of the sampling period h. The main conclusion is that all control systems

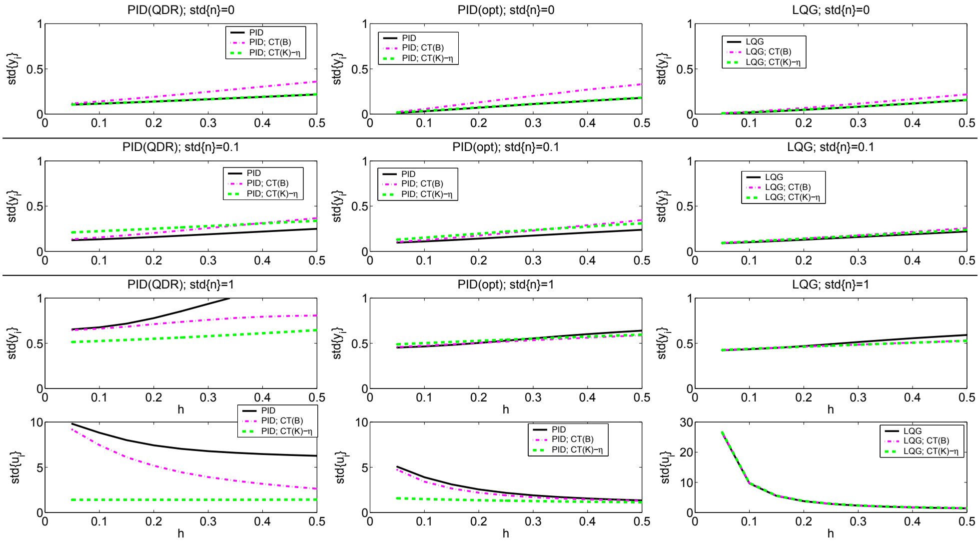

Fig. 6. Control errors and control efforts as functions of h for various noise magnitudes

behave worse when the anti-aliasing filter is used in the noiseless case. This is also true in the case of small noise level and PID controllers.

In contrast to the LQG control, the continuous-time Kalman filter does not help either. Very small improvement is attained in MV LQG system at very high noise level and longer sampling periods. The characteristic feature of MV LQG is that the control magnitudes do not depend on the type of filter used.

The improvement in terms of output variance is better visible in the case of PID controllers. Systems with Kalman filter behave then better in wide range of sampling instants.

Rather large improvement is seen, however, in terms of control signal magnitudes. It does not depend practically on sampling period in the case of CT Kalman filter, and tends to it with increasing sampling period in the case of Butterworth filter.

Selected results for PID and LQG controllers with parameters collected in Table 2 are illustrated in Fig.7 on the plane std$\{u\}$–std$\{y\}$ for $h = 0.2$. It is readily seen that analog filtering makes restricted sense only for PID controllers with QDR tuning and high noise level. Unfortunately the quality of control remains then very poor, even if the continuous-time Kalman filter is applied as analog filter. Application of optimally tuned PID controllers leads to an even more surprising result: from figure Fig.7 it is seen that even at large noise level very good results close to the LQG benchmark can be obtained without any analog filter.

In Fig.7the results are plotted on the plane std$\{u\}$–std$\{y\}$ for various values of h, showing again that the use of anti-aliasing filter makes no sense, and that the quality of disturbance attenuation of optimally tuned PID controllers is very similar to that of MV LQG controller. Unfortunately, Nyquist plots of a series connection of the plant and the controller depicted in Fig.8 show that PID systems are less robust than the MV LQG ones. Moreover, the usage of anti-aliasing filters makes this even worse.

	QDR	std $\{y_i\}$	OPTIMAL	std $\{y_i\}$
	$k_P = 2.8146$		$k_P = 0.9383$	
PID	$T_I = 0.7045$	0.78	$T_I = 0.9647$	0.50
	$T_D = 0.1761$		$T_D = 0.2199$	
	$k_P = 2.2328$		$k_P = 0.9293$	
PID;B	$T_I = 0.8843$	0.71	$T_I = 0.9486$	0.50
	$T_D = 0.2211$		$T_D = 0.2427$	
	$k_P = 1.8621$		$k_P = 1.4118$	
PID;K	$T_I = 1.6319$	0.55	$T_I = 1.5648$	0.53
	$T_D = 0.4080$		$T_D = 0.6619$	

Table 2. QDR PID & Optimal PID controller settings for std $\{n\} = 1$ and $h = 0.2$

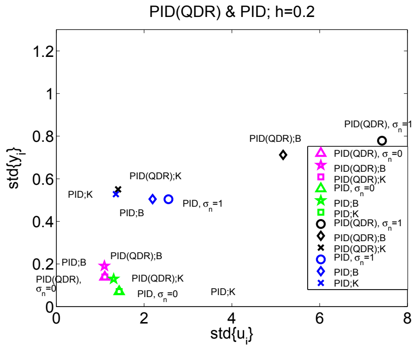

Fig. 7. PID QDR & optimal PID controller results, for $h = 0.2$ with std $\{n(t)\} = 0$ and std $\{n(t)\} = 1$

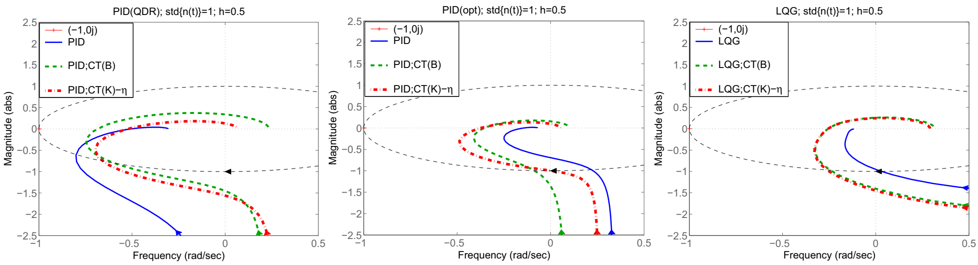

Fig. 8. Nyquist plots and robustness of various control systems

Influence of sampling period and noise character is further studied in figures Fig.9 - Fig.14

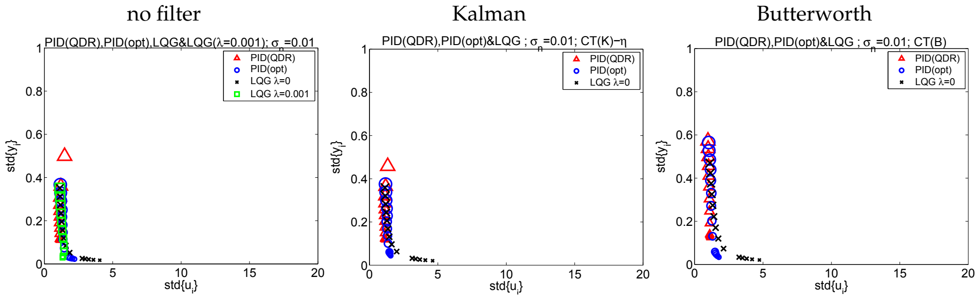

Fig. 9. Negligible noise level results as functions of h, std $\{n_i\} = 0.01$

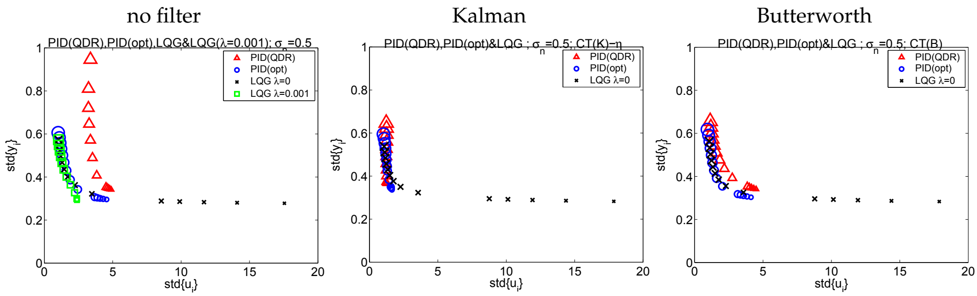

Fig. 10. Wide-band noise results for various controllers and filters as functions of h

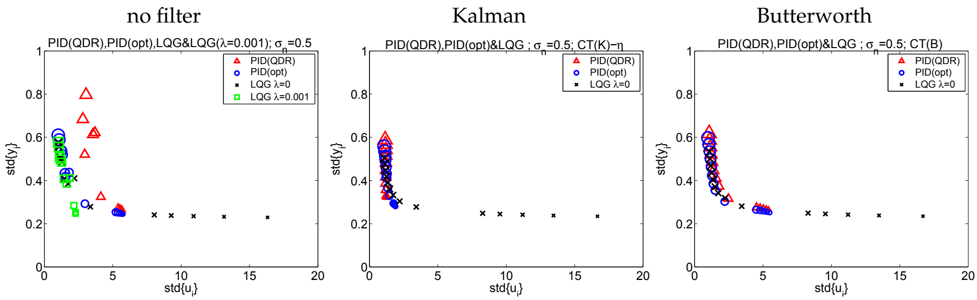

Fig. 11. Mixed-band noise results for various controllers and filters as functions of h

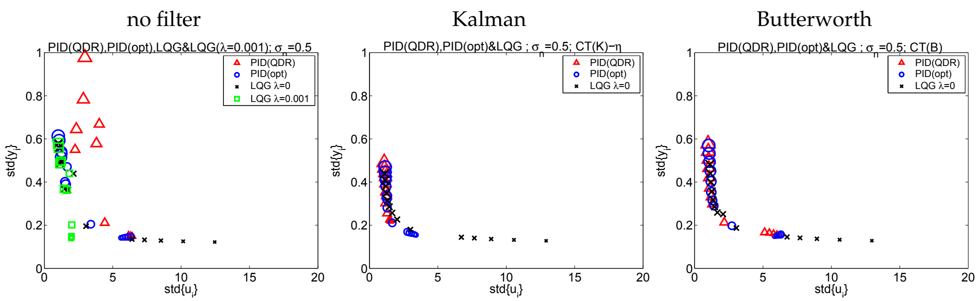

Fig. 12. Narrow-band noise results for various controllers and filters as functions of h

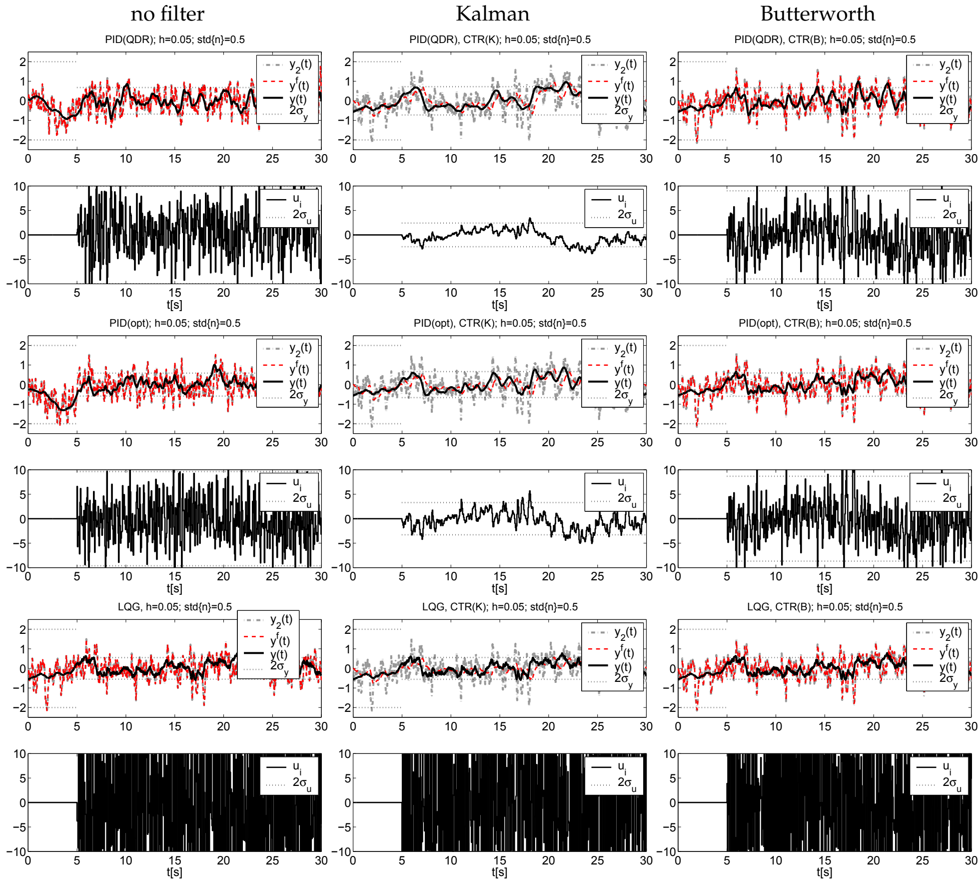

Fig. 13. Wide-band noise: realizations of output and control signals

5. Conclusion

It has been shown that the use of anti-aliasing filters is not justified in sampled-data MV LQG and PID control systems with noiseless measurements, or when the level of noise is small. Certain improvement can be made in the case of PID control systems with QDR and optimal settings in terms of both, output signal and control signal variance, in the case of large level of noise. However, continuous-time Kalman filter is then much better in the wide range of sampling periods, while the effect of Butterworth filter becomes better with increasing sampling period. Unfortunately the usage of any analog filters deteriorates the robustness of control systems. This makes the claim of uselessness of anti-aliasing filters even stronger.
Optimal tuning of PID controllers that takes the disturbance and noise parameters into account leads to the results comparable with those of LQG controllers without any analog prefilters. (Goodwin et al., 2001)

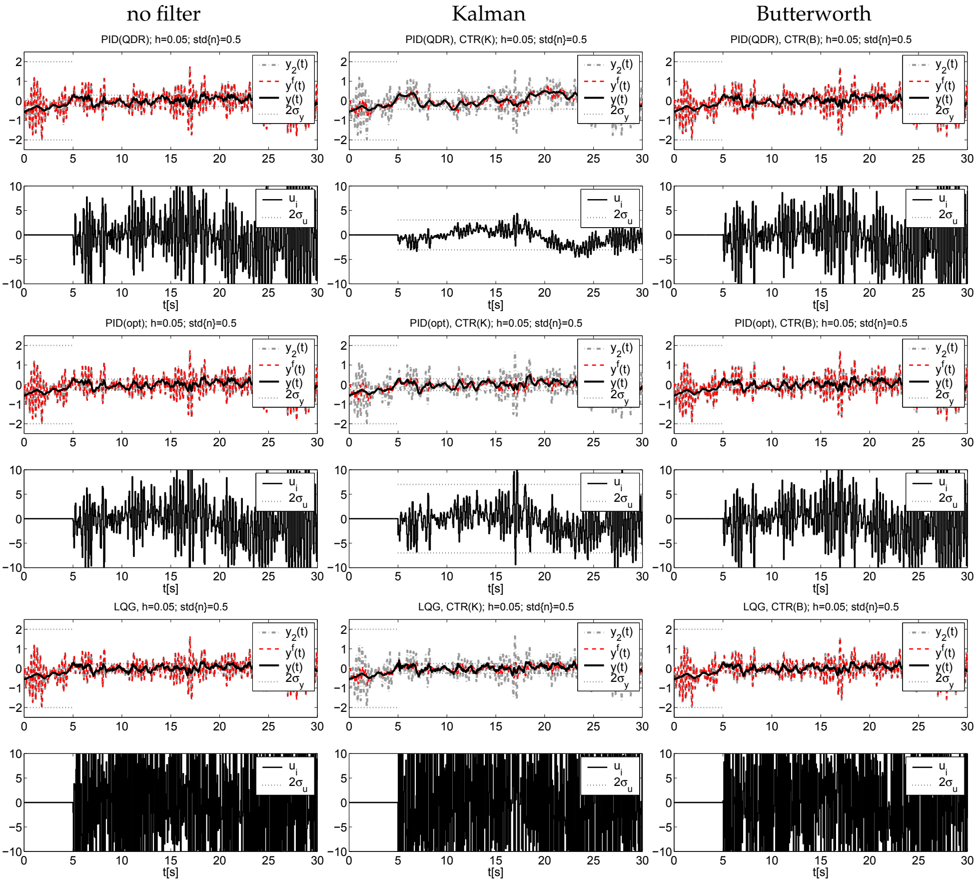

Fig. 14. Narrow-band noise: realizations of output and control signals

6. References

Anderson, B.D.O. and Moore, J.B. (1979). *Optimal Filtering*, Prentice Hall, Inc., Englewood Cliffs, New Jersey, .

Åström, K. and Wittenmark, B. (1997). *Computer–Controlled Systems*, Prentice Hall, 1997.

Blachuta, M. J., Grygiel, R. T. (2008a). Averaging sampling: models and properties. *Proc. of the 2008 American Control Conference*, pp. 3554-3559, Seattle USA, June 2008.

Blachuta, M. J., Grygiel, R. T. (2008b). Sampling of noisy signals: spectral vs anti-aliasing filters, *Proc. of the 2008 IFAC World Congress*, pp. 7576-7581, Seul Korea, July 2008.

Blachuta, M. J., Grygiel, R. T. (2009a). On the Effect of Antialiasing Filters on Sampled-Data PID Control, *Proc. of 21th Chinese Conference on Decision and Control*, Guilin China, June 2009.

Blachuta, M. J., Grygiel, R. T. (2009b). Are anti-aliasing filters really necessary for sampled-data control? *Proc. of the 2009 American Control Coference*, pp. 3200-3205, St Louis USA, June 2009.

Blachuta, M. J., Grygiel, R. T. (2009c). Are anti-aliasing filters necessary for PID sampled-data control? *Proc. of European Control Conference*, Budapest Hungary, August 2009.

Blachuta, M. J., Grygiel, R. T. (2010). Impact of Anti-aliasing Filters on Optimal Sampled-Data PID Control. *Proc. of 8th IEEE International Conference on Control & Automation*, Xiamen China, June 2010.

Feuer, A. and Goodwin, G. (1996). *Sampling in Digital Signal Processing and Control*. Birkhäuser Boston, 1996.

Goodwin, G.C.; Graebe S.F.; and Salgado M.F. (2001). *Control System Design*. Prentice Hall, 2001.

Jerri, A.J. (1977). The Shannon sampling theorem - its variuos extensions and applications: a tutorial review. *Proc. IEEE*, Vol.(65), 1977, pp. 1656-1596

Steinway, W.J. and Melsa, J.L. (1971). Discrete Linear Estimation for Previous Stage Noise Correlation. *Automatica*, Vol. 7, pp. 389-391, Pergamin Press, 1971.

Shats, S. and Shaked U. (1989). Exact discrete-time modelling of linear analogue system. *Int. J. Control*, Vol. 49, No. 1, pp 145-160, 1989.

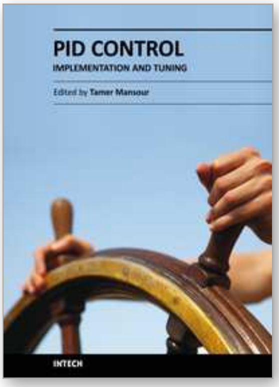

PID Control, Implementation and Tuning

Edited by Dr. Tamer Mansour

ISBN 978-953-307-166-4
Hard cover, 238 pages
Publisher InTech
Published online 19, April, 2011
Published in print edition April, 2011

The PID controller is considered the most widely used controller. It has numerous applications varying from industrial to home appliances. This book is an outcome of contributions and inspirations from many researchers in the field of PID control. The book consists of two parts; the first is related to the implementation of PID control in various applications whilst the second part concentrates on the tuning of PID control to get best performance. We hope that this book can be a valuable aid for new research in the field of PID control in addition to stimulating the research in the area of PID control toward better utilization in our life.